Volume 6 | Number 34 | 14 September 2018 | Pages 9033–9278

Journal of Materials Chemistry C

Materials for optical, magnetic and electronic devices

rsc.li/materials-c

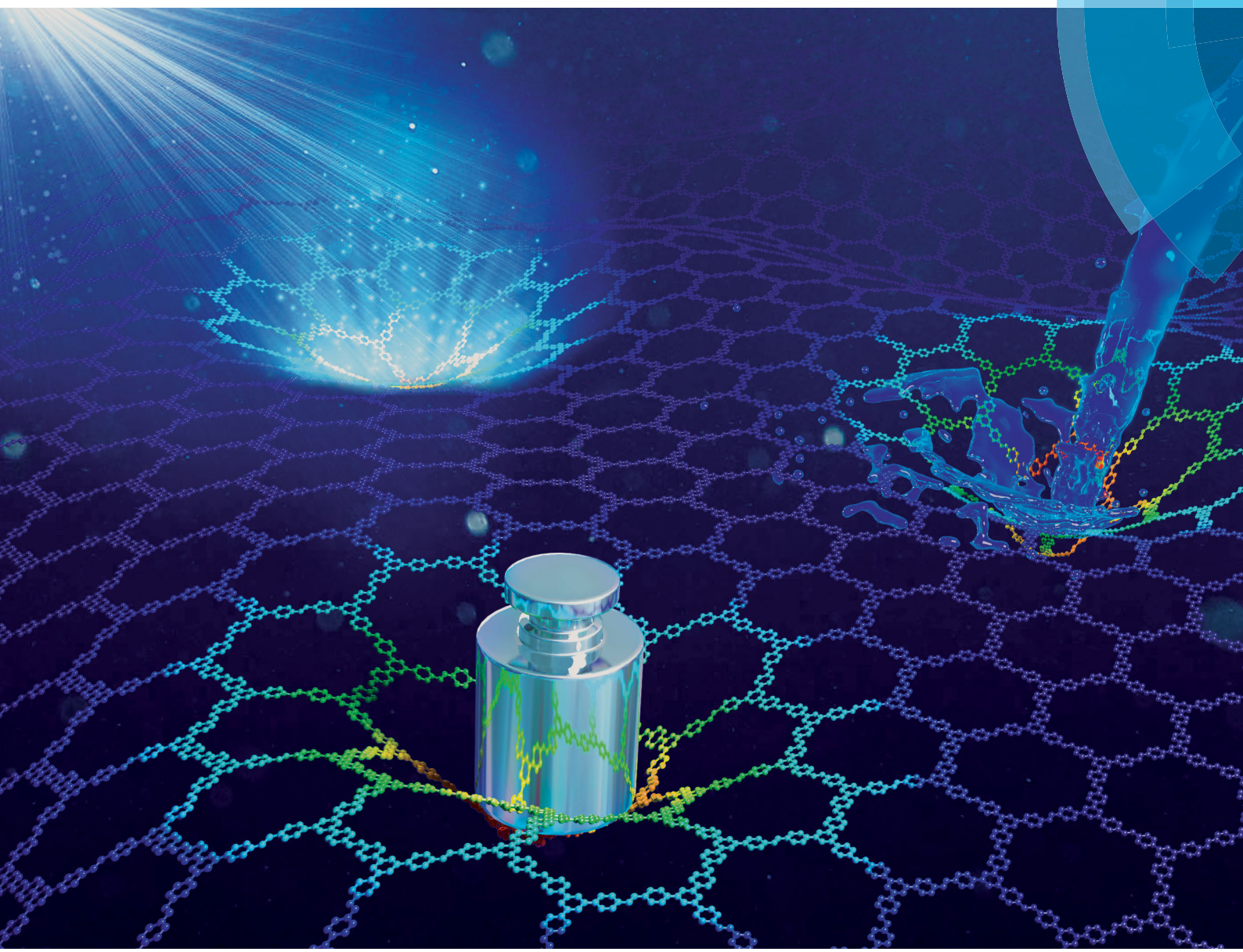

ISSN 2050-7526

ROYAL SOCIETY OF CHEMISTRY

PAPER

Jie Zhang, Jiayin Yuan *et al.*

Three birds, one stone – photo-/piezo-/chemochromism in one conjugated nanoporous ionic organic network

Journal of Materials Chemistry C

PAPER

View Article Online
View Journal | View Issue

Cite this: J. Mater. Chem. C, 2018, 6, 9065

Three birds, one stone – photo-/piezo-/chemochromism in one conjugated nanoporous ionic organic network†

Jian-Ke Sun,‡[a] Ya-Jun Zhang,‡[b] Gui-Peng Yu,[a] Jie Zhang,*[bc] Markus Antonietti[a] and Jiayin Yuan*[ade]

Received 19th March 2018,
Accepted 23rd May 2018

DOI: 10.1039/c8tc01324a

rsc.li/materials-c

A nanoporous material bearing a high ion density and inherent organic radical character was synthesized by a facile one-pot process, which exhibits photo-, piezo- and chemochromism, driven by the diverse electron transfer processes between the acceptor framework and different electron donors. The responsive behavior is useful for its sensing application, as demonstrated here for pressure, anion and gas sensing.

Introduction

Nanoporous polymeric networks (NPNs) combine the principles of designable functional organic groups and the effects of physical nanoconfinement and hold great promise for engineering stimuli-responsive materials.[1] For example, one approach to produce photo-responsive NPN materials is to immobilize photoactive chromophores onto the porous skeleton, in which the pore and its corresponding properties could be switched between different conformation/chemical states by photostimuli.[2] Besides, the co-existence of a photoresponsive unit in the porous network capable of undergoing a chemical reaction allows preparation of dual-stimuli responsive NPNs, as demonstrated recently in two spiropyran-functionalized porous aromatic networks, which reacted reversibly to photo/chemical stimuli.[3] Meanwhile, there is a natural tendency to pursue multi-stimuli responsive materials that enhance their usefulness in multifarious applications.[4] Access to materials that are porous and multi-responsive is nevertheless challenging with rare examples of multi-stimuli responsive NPNs reported.[4] An associated difficulty is to find a wise choice of the building units and their spatial assembly in porous skeletons that govern more than one type of adaptive chemistries to achieve controlled switching properties in the solid state.

Recently, nanoporous ionic organic networks (NIONs) bearing covalently tethered cations and/or anions have emerged as a new class of functional materials.[5] Compared with the neutral counterparts, the ions in NIONs increase the adsorbate–adsorbent interaction through polarization effects and coulombic forces,[6] and provide dynamic ionic bonds in the host skeleton to modify framework properties by the experimentally easy-to-perform ion exchange reaction.[7] In some cases, ion pairs may couple electronically to a conjugated polymer framework to enhance its ion conductivity or enable exotic photoelectrochemical properties.[8] Recent observations indicated that high ion density in a conjugated skeleton may promote or bias the internal electron/hole mobility due to charge delocalization effects.[9] Inspired by these findings, NIONs are considered as a useful structural toolbox for engineering "smart" materials.

Herein, we report a built-in pyridinium chloride-based NION (termed NION-Cl) consisting of a triazine core and a 1,2-bis-(4-pyridinium)ethylene (4,4′-bpe) branch. The electron-deficient pyridinium cation[10] has been often used to construct functional organic or metal–organic hybrid materials.[11] By integrating pyridinium cations into an organic aromatic skeleton, we observed enhanced photoelectrochemical redox activity, which in combination with the nanopores endows NION-Cl with reversible photo-, piezo- and chemochromism (the latter including solvo-, aniono- and vapochromism).

[a] Max-Planck-Institute of Colloids and Interfaces, D-14476 Potsdam, Germany. E-mail: jiayin.yuan@mpikg.mpg.de
[b] State Key Laboratory of Structural Chemistry, Fujian Institute of Research on the Structure of Matter, The Chinese Academy of Sciences, Fuzhou, Fujian 350002, P. R. China
[c] MOE Key laboratory of Cluster Science, Beijing Key Laboratory of Photoelectronic/Electrophotonic Conversion Materials, School of Chemistry and Chemical Engineering, Beijing Institute of Technology, Beijing, P. R. China
[d] Department of Chemistry & Biomolecular Science& Center for Advanced Materials Processing (CAMP), Clarkson University, 8 Clarkson Avenue, Potsdam, New York 13699, USA
[e] Department of Materials and Environmental Chemistry, Stockholm University, Svante Arrhenius väg 16 C, 10691 Stockholm, Sweden. E-mail: jiayin.yuan@mmk.su.se

† Electronic supplementary information (ESI) available: Additional characterization of NIONs and their application. See DOI: 10.1039/c8tc01324a

‡ These authors contributed equally to this work.

Results and discussion

NION-Cl was readily synthesized in one-pot *via* nucleophilic substitution of 2,4,6-trichloro-1,3,5-triazine with 4,4′-bpe in ethyl acetate at 100 °C (Scheme 1). A yellowish brown product insoluble in organic solvents was obtained at a high yield of >90% after purification with multiple steps of solvent (ethyl acetate) washing. Its Fourier transform infrared (FT-IR) spectrum was recorded and compared to its two precursors *i.e.* 2,4,6-trichloro-1,3,5-triazine with 4,4′-bpe (details in Fig. S1–S3, ESI†), confirming the larger extent of the nucleophilic substitution reaction. The chemical structure of NION-Cl was investigated by solid-state ^{13}C cross-polarization magic angle spinning nuclear (^{13}C CP-MAS NMR) spectroscopy (Fig. S4, ESI†). In detail, the signal at 160.1 ppm is assigned to the triazine carbons,[12,13] while signals for pyridine and pyridinium carbons range from 147.3 to 121.1 ppm.[5b] Based on their integration ratios, part of the 4,4′-bpe linkers must be in a reduced state. Here, according to the measured total Cl content (17.76 wt%) by combustion elemental analysis and the Cl^- content by the anion exchange experiment showing that nearly half of the Cl^- has left the network, it is concluded that each linker unit has one of its two pyridinium chloride moieties in the intermediate reduced state (Scheme 1, details in the ESI†). This is similar to the findings by Bourlinos *et al.* who synthesized an analogous but nonporous framework polymer and observed spontaneous reduction and chlorine depletion to be about 50%.[11c] TGA-DSC analysis revealed that the current network is stable up to 240 °C (Fig. S5, ESI†).

In the scanning electron microscopy (SEM) image (Fig. 1a), NION-Cl exists in the form of primary precipitated particles of 0.5–3 μm in size, which aggregate irregularly into an aerogel-like structure. Energy-dispersive X-ray spectroscopy (EDX) mapping determines the presence of the component elements of C, N, and Cl, which are homogeneously distributed in the network (Fig. 1b–d). Powder X-ray diffraction (XRD) measurements reveal its amorphous state (Fig. S6, ESI†). The N_2 sorption isotherm of NION-Cl shows a moderate Brunauer–Emmett–Teller (BET) surface area of 75 $m^2\ g^{-1}$ (Fig. S7, ESI†) with a sharp N_2 uptake at $p/p_0 \sim 0.9$, indicative of large mesopores that are confirmed by the pore size distribution plot shown in Fig. S8 (ESI†). As reported previously in ionic

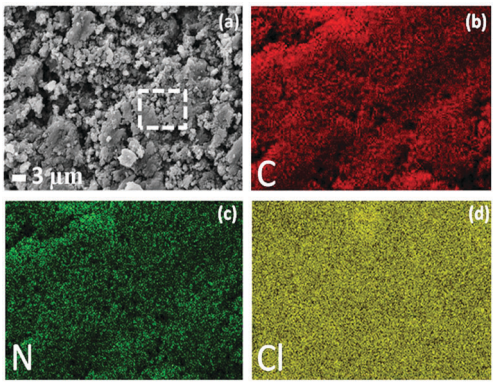

Fig. 1 (a) SEM image and (b–d) the corresponding EDX mapping of elements C (red), N (green), and Cl (yellow) in NION-Cl.

metal–organic frameworks (MOFs),[10] ionic pairs on the pore wall generate highly polarized, energetic binding sites that preferentially adsorb polar molecules. It is assumed that in NION-Cl the involved high interface energy collapsed the polymer pores throughout solvent removal by high-vacuum thermo-drying, but solvents of high polarity may enter and reopen these pores. Indeed, NION-Cl selectively takes up more polar vapors, *e.g.*, water (216 mg g^{-1}) and alcohols (methanol: 81 mg g^{-1}, ethanol: 42 mg g^{-1}), while nonpolar ones like cyclohexane only bind to the outer surface (10 mg g^{-1}) (Fig. 2). The pore size as revealed by the hysteresis of water sorption experiments nicely coincides with the geometric expectations from the structural model.

Photochromism was observed when irradiating NION-Cl under a xenon lamp (200 mW cm^{-2}) at room temperature (RT). A color evolution from yellowish brown to pale violet was spotted in 2 min (Fig. 3a). Continuous irradiation deepens its color to dark violet in 2 h (Fig. 3a). In this process, the photo-induced [2+2] cycloaddition reaction typical for 4,4′-bpe was excluded as no change of the C=C vibration signal was detected by IR (Fig. S1, ESI†) and Raman spectroscopy (Fig. S9, ESI†). Photo-induced *cis–trans* transformation is negligible as no band shift of the olefin group (~320 nm) was spotted after coloration (Fig. 3b), perhaps due to steric hindrance, *i.e.* the chains are locked by covalent crosslinks. By contrast, the native 4,4′-bpe

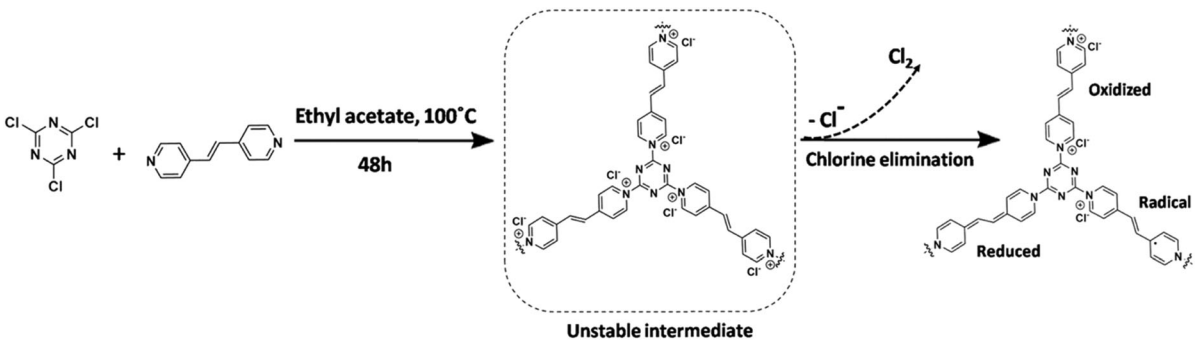

Scheme 1 Chemical structures and the synthetic route to NION-Cl bearing a pyridinium chloride ion pair. In the first step, a system with two cations per 4,4′-bpe-linker is formed (unstable intermediate), which is so electron-deficient that it is spontaneously reduced[11c] to the well-known mono-cation-radical under elimination of elemental chlorine. The diagram indicates three possible states: oxidized, reduced, and the monoradical which can disproportionate in the "redox-state". Note that the central double bond favors stabilization of all 3 states.

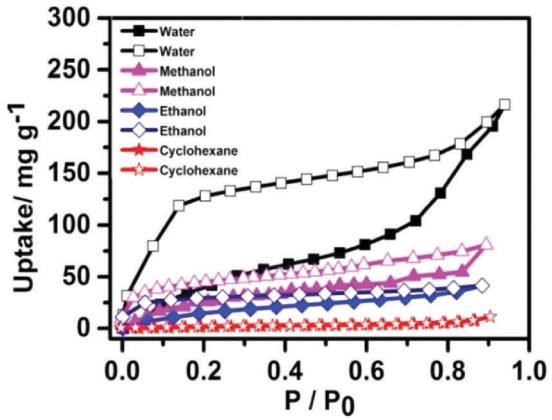

Fig. 2 Sorption isotherms of NION-Cl toward different vapors at 298 K. Solid symbols for the adsorption branch and hollow ones for the desorption branch.

monomer undergoes a *trans–cis* isomerization after irradiation under the same conditions (Fig. S10, ESI†).[14] In the UV-Vis diffuse reflectance spectra, photoirradiation creates broad absorption bands in 440–800 nm with a shoulder at 740 nm. Such photo-induced absorption changes are similar to a previous observation in well-studied 4,4′-bipyridinium (viologen) derivatives,[15] while these changes are rarely observed in 4,4′-bpe derivatives in the solid state.[16] The UV-Vis spectrum of the irradiated sample is highly similar to that of the *N*-methyl-4-[*trans*-2-(4-pyridyl)ethenyl] radical (Mebpe) obtained by electrochemical reduction in solution,[17] which points to the stable radical state of the irradiated sample.

Photochromism was interpreted as the transfer of the redox linkers in NION-Cl into stable monoradicals by photo-induced electron transfer (ET). The existence of free radicals is confirmed by electron spin resonance (ESR) spectroscopy measurements (Fig. 3c), in which the signal (g = 2.003) right after coloration is massively amplified. Such a process was rarely observed in solid-state 4,4′-bpe derivatives, but it resembles the common photochromism and photogeneration of free radicals in 4,4′-bipyridinium derivatives.[15] The dark violet color upon prolonged irradiation is consistent with the build-up of radical concentration in NION-Cl (Fig. S11, ESI†), also underlining the metastability of the poly-radical species. Note that already before irradiation, a radical signal at the same position exists, indicating the presence of a moderate radical species in the sample when synthesized, as shown in Scheme 1.

The concentration and stability of the radicals seem to be high enough that XPS measurements can characterize and differentiate the original and irradiated samples (Fig. 4). Notable shifts of the binding energy in both the Cl 2p and N 1s spectra after irradiation can be observed. In the native sample, the N 1s core-level spectrum can be fitted to two peaks at 400.2 and 398.1 eV attributed to the N atoms of the pyridine/pyridinium and triazine systems, respectively (Fig. 4a). After coloration, a new peak emerged at a lower binding energy (398.9 eV) due to the photo-induced partial reduction of pyridinium nitrogen

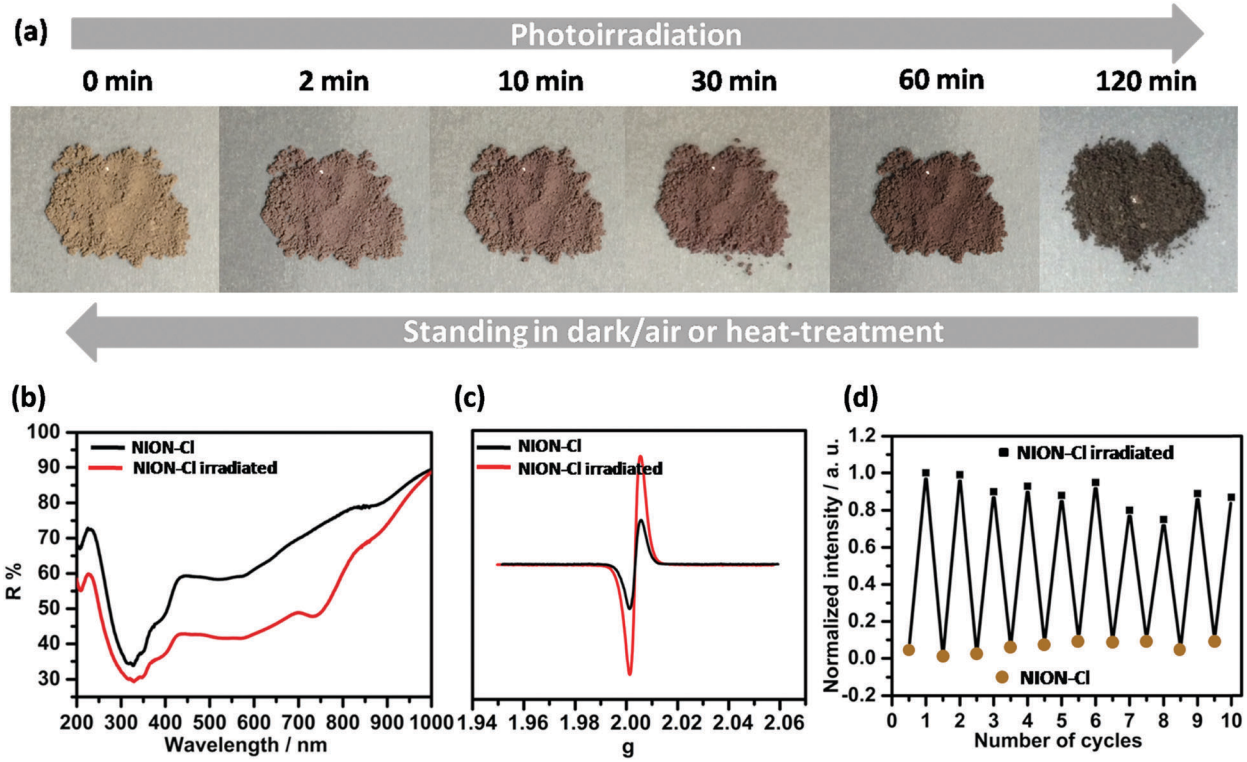

Fig. 3 (a) Time dependent coloration of NION-Cl under a Xe lamp (200 mW cm^{-2}) and its reversible process by storage in air in the dark, a process that can be accelerated by thermal-treatment. (b) The UV-Vis diffuse reflectance spectra and (c) the ESR signal before and after photoirradiation. (d) Absorbance at λ = 740 nm in repeated coloring and bleaching cycles.

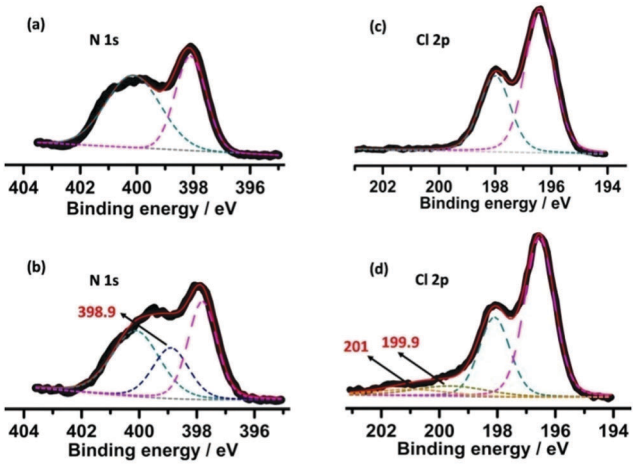

Fig. 4 XPS core-level spectra of N 1s and Cl 2p before (a and c) and after (b and d) photoirradiation. The dashed lines depict the resolved peaks, the sum of which is shown by a red solid line.

cations (Fig. 4b). The Cl spectra similarly reveal: besides Cl^- (Cl $3d_{5/2}$ and $3d_{3/2}$ at 196.6 and 198.1 eV, respectively, Fig. 4c), in the photoirradiated sample two new peaks at 199.9 and 201 eV appeared (Fig. 4d) that stem from the partial generation of electrostatically neutral chlorine,[15a] suggesting that some Cl^- anions lost electrons upon photoirradiation and are involved in radical stabilization.

Based on the evidence, the ET process is believed to be shuttled between the electron-rich Cl^- anion and the electron-deficient pyridinic N^+ cation radical, similar to the previously reported metal–bipyridinium hybrids.[15] Shuttling by the Cl-radical occurs going from a linker-to-linker unit, leading to equilibration. Further proof is provided by a control experiment by exchanging Cl^- with BF_4^- (Fig. S12, ESI†) that is of lower electrochemical activity. The resultant material is ''photo-inert'' and does not change its color under the same conditions due to the lack of Cl^- that forbids the aforementioned ET process. It is worth mentioning that the photochromism is reversible (Fig. 3a and d) upon storage of the sample in the dark for days at RT, suggesting the acceleration effect of oxygen on free radical quenching despite the fact that the reversible back electron transfer from pyridinium to Cl^- may occur.[11a] Such a process can be further accelerated by annealing at 100 °C.

Interestingly, NION-Cl is also sensitive to pressure (piezochromism). In Fig. 5a, NION-Cl in a disc shape gradually deepens its color under an external mechanical pressure from 0 to 9 MPa. The IR spectra before and after the pressing treatment show little-to-no difference (Fig. S13, ESI†), indicating its chemical structural stability upon such a treatment. In combination with ESR (Fig. 5b), UV-Vis (Fig. S14, ESI†), and XPS analyses (Fig. S15, ESI†), piezochromism was identified to follow a similar ET process as discussed above for photochromism. The piezochromism however cannot be quickly reversed by releasing the exerted external pressure alone, as it is stable in air at least for several weeks, implying that radicals created by mechanical forces are locked due to perhaps a deformed metastable state of the porous framework. Considering that the

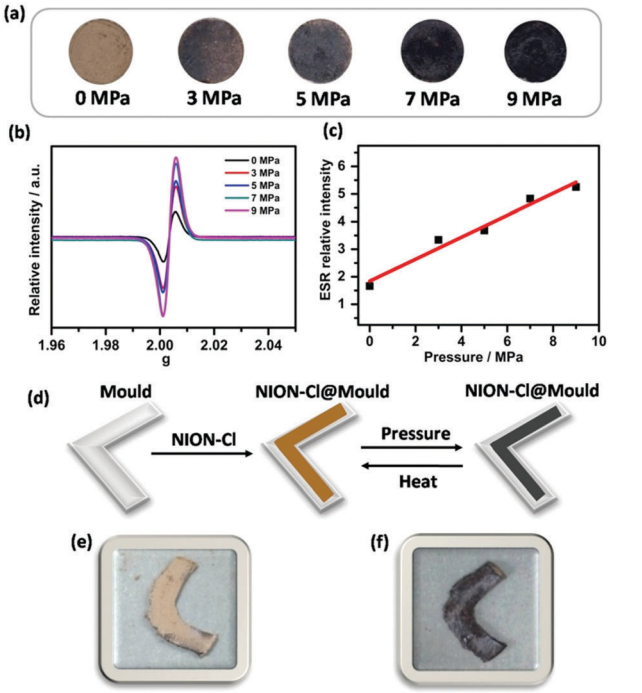

Fig. 5 (a) Pressure dependent coloration of a NION-Cl disk. (b) ESR signals for the corresponding disk. (c) Plot of ESR intensity *vs.* external pressure. (d–f) Schematic illustration and real samples of the mould-assisted casting method to show the ''pressure memory'' effect of NION-Cl.

external mechanical pressure is in a quasi-linear relationship to the detected ESR intensity (Fig. 5c), NION-Cl is expected to serve as a pressure sensor or a ''pressure memory'' material.[18] For example, NION-Cl plastics can be processed by the mould casting technique (Fig. 5d–f), and the color of the product can ''visualize'' the maximum pressure exerted on itself during processing.

NION-Cl shows chemochromism as well. In this context, three types of chemical stimuli *i.e.* solvent, anion and vapor were employed. Solvochromism took place in CH_3CN, in which NION-Cl turned dark brown, a state that can be reversed by vacuum and thermal-treatment of the sample to remove CH_3CN (evidenced in the IR spectra in Fig. S16 (ESI†) that show no CH_3CN residue bands). It did not occur in other solvents tested, *e.g.*, THF, acetone, ether, cyclohexane, MeOH or EtOH (Fig. 6a). CH_3CN was obviously able to stabilize the monoradical state of the framework in the charge delocalized skeleton. This hypothesis was supported by XPS measurements, which shows a typical binding energy shift of the N 1s core spectrum (Fig. S17, ESI†); meanwhile, the Cl 2p core peak remains the same, as shown in Fig. S18 (ESI†). The generated free radical accounting for solvochromism was further evidenced by UV-Vis and ESR spectra (plots and discussion in Fig. S19 and S20, ESI†).

Similarly, NION-Cl exhibits anionochromism in contact with strong electron donating anions, here dicyanamide ($N(CN)_2^-$, 0.01 M in ethanol). $N(CN)_2^-$ changes NION-Cl from yellowish brown to dark brown *via* a spontaneous ET process similar to that in photochromism, which was demonstrated by the data collected from and discussion conducted on the IR, UV-Vis, ESR

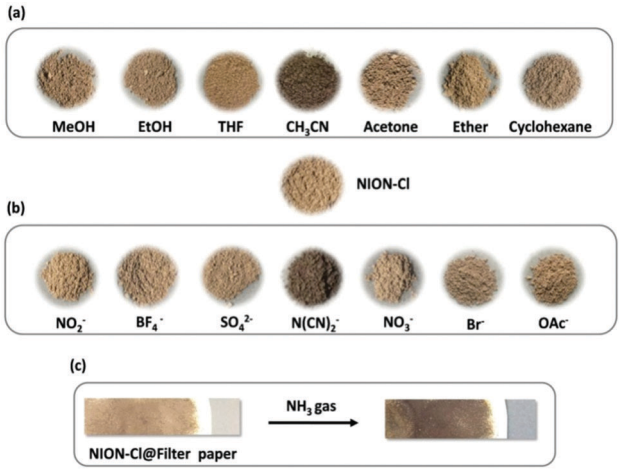

Fig. 6 Chemochromism of NION-Cl. (a) Solvochromism in CH_3CN, (b) anionochromism toward $N(CN)_2^-$ anion, and (c) vapochromism towards NH_3.

and XPS spectra shown in Fig. S21 and S24 (ESI†). In contrast other anions, *e.g.* SO_4^{2-}, BF_4^-, NO_3^- OAc^-, NO_2^- or F^- failed (Fig. 6b). The significance is that the threshold $N(CN)_2^-$ concentration that can deliver a clear message of coloration for a detectable anionochromism goes as low as 10 ppm (Fig. S25, ESI†), and the colored state can last for a long time, which positions NION-Cl in the sensory range for $N(CN)_2^-$ detection. Moreover, vapor can be a stimulus as well. NION-Cl fine powers casted into a white filter paper (NION-Cl@filter paper) features vapochromism and turns deep brown in contact with NH_3 gas at a concentration above 100 ppm (Fig. 6c). Here, the NH_3 molecule is expected to act as the radical stabilizer, as reported in the literature[19] and evidenced here by Raman, UV-Vis, ESR and XPS measurements in Fig. S26 and S29 (ESI†). Such a colored state is stable in air but can be resorted by the removal of NH_3 *via* thermal treatment.

Conclusions

In conclusion, a pyridinium chloride-based conjugated NION in a mixed reduced/oxidized framework state was synthesized which was able to convert itself into a polyradical state in response to external stimuli. It can exhibit photo-, piezo- and chemochromism *via* an ET process from linker to linker that is associated with accumulated synproportionation of the structure, generating free radicals in the porous network. Given their reversible behavior, such NIONs are candidates for stable sensing in diverse physical/chemical environments. The versatile function and performance in combination with the ease of synthesizing NION-Cl suggest a robust pathway for future engineering of "smart" porous materials.

Conflicts of interest

There are no conflicts of interest to declare.

Acknowledgements

J. Y. acknowledges financial support from the Max Planck Society, the ERC Starting Grant (639720-NAPOLI) and a startup Grant from Clarkson University. The authors acknowledge the Wallenberg Academy Fellowship program KAW2017.0166 from the Knut and Alice Wallenberg Foundation. J. K. S. thanks the Alexander von Humboldt (AvH) Foundation. J. Z. acknowledges the National Natural Science Foundation of China (Grant No. 21573016/21403241). Open Access funding provided by the Max Planck Society.

Notes and references

1 (*a*) R. Dawson, A. I. Cooper and D. J. Adams, *Prog. Polym. Sci.*, 2012, **37**, 530–563; (*b*) N. B. McKeown and P. M. Budd, *Chem. Soc. Rev.*, 2006, **35**, 675–683; (*c*) A. Thomas, *Angew. Chem., Int. Ed.*, 2010, **49**, 8328–8344; (*d*) D. Wu, F. Xu, B. Sun, R. Fu, H. He and K. Matyjaszewski, *Chem. Rev.*, 2012, **112**, 3959–4015; (*e*) S. Das, P. Heasman, T. Ben and S. Qiu, *Chem. Rev.*, 2017, **117**, 1515–1563; (*f*) S. Kandambeth, A. Mallick, B. Lukose, M. V. Mane, T. Heine and R. Banerjee, *J. Am. Chem. Soc.*, 2012, **134**, 19524–19527; (*g*) K. Wang, L. Yang, X. Wang, L. Guo, G. Cheng, C. Zhang, S. Jin, B. Tan and A. I. Cooper, *Angew. Chem., Int. Ed.*, 2017, **56**, 14149–14153; (*h*) F. Vilela, K. Zhang and M. Antonietti, *Energy Environ. Sci.*, 2012, **5**, 7819–7832; (*i*) H. Bildirir, V. G. Gregoriou, A. Avgeropoulos, U. Scherfd and C. L. Chochos, *Mater. Horiz.*, 2017, **4**, 546–556.

2 M. Baroncini, S. d'Agostino, G. Bergamini, P. Ceroni, A. Comotti, P. Sozzani, I. Bassanetti, F. Grepioni, T. M. Hernandez, S. Silvi, M. Venturi and A. Credi, *Nat. Chem.*, 2015, **7**, 634–640.

3 P. K. Kundu, G. L. Olsen, V. Kiss and R. Klajn, *Nat. Commun.*, 2014, **5**, 3588.

4 (*a*) M. A. C. Stuart, W. T. S. Huck, J. Genzer, M. Müller, C. Ober, M. Stamm, G. B. Sukhorukov, I. Szleifer, V. V. Tsukruk, M. Uurban, F. Winnik, S. Zauscher, I. Luzinov and S. Minko, *Nat. Mater.*, 2010, **9**, 101–113; (*b*) Y. X. Ma, Z. J. Li, L. Wei, S. Y. Ding, Y. B. Zhang and W. Wang, *J. Am. Chem. Soc.*, 2017, **139**, 4995–4998.

5 (*a*) J. K. Sun, M. Antonietti and J. Yuan, *Chem. Soc. Rev.*, 2016, **45**, 6627–6656; (*b*) P. Zhang, Z. Qiao, X. Jiang, G. M. Veith and S. Dai, *Nano Lett.*, 2015, **15**, 823–828; (*c*) S. Zhang, K. Dokko and M. Watanabe, *Chem. Sci.*, 2015, **6**, 3684–3691; (*d*) J. Byun, H. A. Patel, D. Thirion and C. T. Yavuz, *Polymer*, 2017, **126**, 308–313.

6 (*a*) B. Li, Y. Zhang, D. Ma, Z. Shi and S. Ma, *Nat. Commun.*, 2014, **5**, 5537; (*b*) W. Lu, D. Yuan, J. Sculley, D. Zhao, R. Krishna and H. C. Zhou, *J. Am. Chem. Soc.*, 2011, **133**, 18126–18129; (*c*) S. Subramanian, J. Park, J. Byun, Y. Jung and C. T. Yavuz, *ACS Appl. Mater. Interfaces*, 2018, **10**, 9478–9484.

7 (*a*) Y. Yuan, F. X. Sun, L. Li, P. Cui and G. S. Zhu, *Nat. Commun.*, 2014, **5**, 4260; (*b*) O. Buyukcakir, S. H. Je, D. S. Choi, S. N. Talapaneni, Y. Seo, Y. Jung, K. Polychronopoulouc and A. Coskun, *Chem. Commun.*, 2016, **52**, 934–937; (*c*) G. Das,

T. Prakasam, S. Nuryyeva, D. S. Han, A. Abdel-Wahab, J. C. Olsen, K. Polychronopoulou, C. PlatasIglesias, F. Ravaux, M. Jouiad and A. Trabolsi, *J. Mater. Chem. A*, 2016, **4**, 15361–15369; (*d*) P. Zhang, X. Jiang, S. Wan and S. Dai, *Chem. – Eur. J.*, 2015, **21**, 12866–12870.

8 (*a*) Y. Zhang, A. Thomas, M. Antonietti and X. Wang, *J. Am. Chem. Soc.*, 2009, **131**, 50–51; (*b*) P. Zhang, M. Li, B. Yang, Y. Fang, X. Jiang, G. M. Veith, X. G. Sun and S. Dai, *Adv. Mater.*, 2015, **27**, 8088–8094; (*c*) S. Ghasimi, S. Prescher, Z. J. Wang, K. Landfester, J. Yuan and K. A. I. Zhang, *Angew. Chem., Int. Ed.*, 2015, **54**, 14549–14553.

9 (*a*) U. Scherf, *Angew. Chem., Int. Ed.*, 2011, **50**, 5016–5017; (*b*) C. Gu, N. Huang, Y. Chen, H. Zhang, S. Zhang, F. Li, Y. Ma and D. Jiang, *Angew. Chem., Int. Ed.*, 2016, **55**, 3049–3053; (*c*) C. R. Mulzer, L. Shen, R. P. Bisbey, J. R. McKone, N. Zhang, H. D. Abruña and W. R. Dichtel, *ACS Cent. Sci.*, 2016, **2**, 667–673.

10 J. K. Sun, X. D. Yang, G. Y. Yang and J. Zhang, *Coord. Chem. Rev.*, 2017, DOI: 10.1016/j.ccr.2017.10.029.

11 (*a*) C. Chen, J. K. Sun, Y. J. Zhang, X. D. Yang and J. Zhang, *Angew. Chem., Int. Ed.*, 2017, **46**, 14458–14462; (*b*) A. J. Bard and M. A. Fox, *Acc. Chem. Res.*, 1995, **28**, 141–145; (*c*) A. B. Bourlinos, P. Dallas, Y. Sanakis, D. Stamopoulos, C. Trapalis and D. Niarchos, *Eur. Polym. J.*, 2006, **42**, 2940–2948; (*d*) G. Das, T. Skorjanc, S. K. Sharma, F. Gándara, M. Lusi, D. S. S. Rao, S. Vimala, S. K. Prasad, J. Raya, D. S. Han, R. Jagannathan, J. C. Olsen and A. Trabolsi, *J. Am. Chem. Soc.*, 2017, **139**, 9558–9565; (*e*) O. Buyukcakir, S. H. Je, S. N. Talapaneni, D. Kim and A. Coskun, *ACS Appl. Mater. Interfaces*, 2017, **9**, 7209–7216; (*f*) A. A. Rajaa and C. T. Yavuz, *RSC Adv.*, 2014, **4**, 59779–59784.

12 R. D. Chambers, R. S. Matthews, W. K. R. Musgrave and P. G. Urben, *Org. Magn. Reson.*, 1980, **13**, 363–367.

13 (*a*) V. S. Vyas, F. Haase, L. Stegbauer, G. Savasci, F. Podjaski, C. Ochsenfeld and B. V. Lotsch, *Nat. Commun.*, 2015, **6**, 8508; (*b*) M. G. Schwab, B. Fassbender, H. W. Spiess, A. Thomas, X. Feng and K. Mullen, *J. Am. Chem. Soc.*, 2009, **131**, 7216–7217; (*c*) H. A. Patel, F. Karadas, A. Canlier, J. Park, E. Deniz, Y. Jung, M. Atilhan and C. T. Yavuz, *J. Mater. Chem.*, 2012, **22**, 8431–8437.

14 M. K. Itokazu, A. S. Polo, D. L. A. de Faria, C. A. Bignozzi and N. Y. M. Iha, *Inorg. Chim. Acta*, 2001, **313**, 149–155.

15 (*a*) J. Zhang, M. M. Matsushita, X. X. Kong, J. Abe and T. Iyoda, *J. Am. Chem. Soc.*, 2001, **123**, 12105–12106; (*b*) M. S. Wang, C. Yang, G. E. Wang, G. Xu, X. Y. Lv, Z. N. Xu, R. G. Lin, L. Z. Cai and G. C. Guo, *Angew. Chem., Int. Ed.*, 2012, **51**, 3432–3435.

16 Y. J. Zhang, C. Chen, B. Tan, L. X. Cai, X. D. Yang and J. Zhang, *Chem. Commun.*, 2016, **52**, 2835–2838.

17 M. Busby, F. Hartl, P. Matousek, M. Towrie and A. Vlček, Jr., *Chem. – Eur. J.*, 2008, **14**, 6912–6923.

18 H. Narayana, J. Hu, B. Kumar, S. Shang, J. Han, P. Liu, T. Lin, F. Jia and Y. Zhu, *J. Mater. Chem. B*, 2017, **5**, 1905–1916.

19 M. Leroux, N. Mercier, M. Allain, M. C. Dul, J. Dittmer, A. H. Kassiba, J. P. Bellat, G. Weber and I. Bezverkhyy, *Inorg. Chem.*, 2016, **55**, 8587–8594.

